2005

Aerodynamic Methods for Estimating Turbulent Fluxes

John H. Prueger
USDA-ARS-NSTL

William P. Kustas
USDA-ARS

18 Aerodynamic Methods for Estimating Turbulent Fluxes

JOHN H. PRUEGER
USDA Agricultural Research Service
National Soil Tilth Laboratory
Ames Iowa

WILLIAM P. KUSTAS
USDA Agricultural Research Service
Hydrology Laboratory
Beltsville, Maryland

FLUX GRADIENT APPROACHES

The exchange of energy and mass between a surface and the lowest region of the troposphere is a complex process that governs many hydrological, agricultural, and atmospheric processes. The layer of air directly affected by surface–atmosphere exchanges is strongly influenced by turbulent processes at the surface–atmosphere boundary and extends upward into the atmosphere to a height of approximately 1 km. This region is commonly referred to as the atmospheric boundary layer (ABL) that is uniquely characterized by turbulence resulting from mechanical (wind shear) and buoyancy (thermal) forces at or near the surface. Methods have been developed to evaluate energy/mass (heat, water vapor, trace gases, and pollutants) exchanges between the ABL and the underlying surface. In this chapter, we describe the flux gradient approach for estimating mass and energy fluxes under the rubric of aerodynamic methods. We provide some historical perspective, present fundamental equations in the context of Monin-Obukhov similarity theory and introduce recent developments of an alternative method to compute heat and water vapor fluxes using turbulence variance statistics.

The aerodynamic method necessitates the existence of a relationship between a flux density (mass/energy per unit area per unit time) of an atmospheric constituent and its mass or scalar gradient above a surface and is recognized in the literature as the flux-gradient technique. The early basis for this approach originated from a German physician, Adolph Fick, who in 1855 at the age of 26 proposed a mathematical concept for molecular diffusion using Fourier's theory of heat equilibrium. The resulting statement put forth the physically sound and logical idea that diffusion is proportional to a concentration gradient. It would be 25 years later before the first experimental proof of this idea

 Micrometeorology in Agricultural Systems, Agronomy Monograph no. 47.

was provided. This concept today is well known as Fick's Law of Diffusion (Fick, 1855). Simply stated, the flux for one-dimensional molecular diffusion can be expressed as

$$J = -D\frac{\partial c}{\partial x} \quad [1]$$

where $\partial c/\partial x$ represents a concentration gradient (M L^{-3}) of a constituent c across a horizontal plane x, D is the molecular diffusivity (L^2 T^{-1}), and the flux J is the quantity of a constituent diffusing through a unit area per unit time (M L^{-2} T^{-1}) where M, L, and T are the appropriate Système International (SI) units of mass, length, and time, respectively. The molecular diffusivity term D, is assumed to contain all of the information pertaining to the random motion of individual molecules as a function of volume, temperature and concentration gradient. Equation [1] is used to describe the molecular mass flow (usually along a horizontal direction) across a unit area in a predefined plane that is proportional to a concentration differential across that plane.

An analogous assumption was made for turbulence that simply applied the concept of Fick's Law from a molecular diffusion case to a turbulent diffusion case involving mass and energy from a surface to an overlying atmosphere. The distinction is based on the vertical turbulent (as opposed to molecular) diffusion of mass or energy that is proportional to a mean concentration gradient and a height dependent turbulent (eddy) diffusivity term. Boussinesq (1877) introduced the concept of an eddy diffusivity by assuming that turbulent stresses in the averaged momentum equations are equal to the product of an eddy diffusivity and a mean strain rate. G.I. Taylor (1915) conducted a pioneering investigation in the transport of a scalar (temperature) and proposed an equation of turbulent transport as (in its original form)

$$\frac{\partial \theta}{\partial t} = \frac{vd}{2}\frac{\partial^2 \theta}{\partial z^2} \quad [2]$$

where θ is air temperature, t is time, ν is the velocity scale in the vertical, d is distance in the horizontal that represents a length from the point of origin to the measured location, and z is the vertical spatial coordinate. By direct analogy to Fourier's heat equation for a solid, $\frac{vd}{2}$ can be related to the density of air (ρ), the specific heat of air (C_p) and an eddy diffusivity term (k) as $k = \rho C_p\, wd/2$. Schmidt (1917) expanded this concept to include other scalar admixtures (Brutsaert, 1982) that subsequently led to the present day generalized flux-gradient form of

$$F(z) = k_i \frac{\partial A_c}{\partial z} \quad [3]$$

where F is the energy (or mass) flux in the vertical, $\partial A_c/\partial z$ is a height dependent concentration gradient for any atmospheric constituent and k_i is the eddy diffusiv-

ity assumed to contain all of the transport processes pertaining to the transport of A_c across a vertical plane z.

Specifically, present day flux-gradient theory has been used to represent the transport of momentum, heat, and water vapor in response to a gradient and eddy diffusivity in the following forms;

$$\tau = \rho_a k_m \frac{\partial u}{\partial z} \quad [4]$$

$$H = \rho_a C_p k_h \frac{\partial \theta}{\partial z} \quad [5]$$

$$E = \rho_a k_q \frac{\partial q}{\partial z} \quad [6]$$

where τ is the surface shear stress (kg m^{-1} s^{-2}), H is the sensible heat flux (W m^{-2}), E is the water vapor flux (kg m^{-2} s^{-1}), ρ_a is air density (kg m^{-3}), C_p is specific heat of air (J kg^{-1} K^{-1}), k_m, k_h, and k_q are eddy diffusivities for momentum, heat, and water vapor, respectively (m^2 s^{-1}). Mass and scalar gradients for momentum, heat, and specific humidity are expressed as $\partial u/\partial z$, $\partial \theta/\partial z$, and $\partial q/\partial z$, respectively. The k_i (where $i = m$, h, or q) term has been identified by various names: eddy viscosity, eddy diffusivity, eddy-transfer coefficient, turbulent-transfer coefficient, and gradient-transfer coefficient (Stull, 1988). The eddy viscosity is not a fluid property as is molecular viscosity, but rather a flow property that is related to the state of turbulence. Collectively, Eq. [4–6] represent first order closure or "k-theory" (Richardson, 1920 cites G.I Taylor as the originator of the k-notation) as the product of a scalar concentration gradient and a turbulent diffusivity (k).

All of the complexities and uncertainties of turbulent transport for momentum, heat, and water vapor are embedded in the k term. This greatly simplifies a complicated and nonlinear process. For the case where transport is dominated by small eddies over a uniform surface with sufficient fetch and steady state conditions (in particular neutral) this approach has been successful. Where surface heterogeneity, advection and non-steady state conditions prevail, the approach becomes less valid, and is problematic to implement.

FUNDAMENTAL STRUCTURE OF THE ATMOSPHERE

Consider the structure of the atmosphere that is affected by conditions at or near the surface. Prandtl (1904) first set forth a concept (for momentum transfer) for the region near a solid wall. Under this concept, horizontal gradients are negligible when compared with vertical gradients. In like fashion, the earth's surface (land or water) can be considered a solid wall thus affecting the lower boundary layer of the atmosphere. The depth of this layer can vary from a few 10s of meters during early morning and nocturnal periods increasing to a kilometer or more during the afternoon periods as a result of strong surface heating. A concise and detailed description of the sub-layers with approximate magnitudes of the thickness of the layers that collectively comprise the lower boundary layer of the

atmosphere is provided by Brutsaert (1982) and is summarized below. It is important to keep in mind that the depth of the ABL changes with the diurnal cycle and thus depths of the sub-layers of the ABL are approximations and can vary according to local variations of surfaces and microclimate.

Beginning at the surface of the earth and moving vertically into the atmosphere is a layer approximately $1.5–3.5_{ho}$ (where $_{ho}$ is a typical or average height (m) of the surface elements, i.e., vegetation or obstacles) in depth commonly referred to as the roughness sub-layer (Fig. 18–1). It also is identified in the literature as the interfacial, viscous, or canopy sub-layer with roughness sub-layer the more recognized term. Extending above the roughness sub-layer 1 to 10 m is the dynamic sub-layer where under neutral conditions, wind speed profiles can be expected to be generally logarithmic. Above the roughness sub-layer, is the surface sub-layer or inner region that extends up to 50 to 100 m where wind speed profiles can also be logarithmic. In general, the depth over where Monin-Obukhov Similarity Theory (MOST, discussed later) is applicable is typically 0.1 Z_{ABL} where Z_{ABL} is the height (m) of the atmospheric boundary layer. Over complex terrain Brutsaert and Sugita (1992) report the upper limit of MOST to be approximately 100 $(z - d_o)/z_{om}$ where d_o and z_{om} are roughness parameters described later in the chapter. Beyond the surface sub-layer for a range between 100 and 1000 m is the outer region or defect sub-layer and finally the "free atmosphere" where the term free refers to that part of the atmosphere that is not influenced directly by surface forcings such as mechanical or buoyancy forces related to turbulence and surface heating generated at the surface.

The region of focus for this topic will be the surface sub-layer that is fully turbulent and begins above the roughness sub-layer (nominally three times the height of surface obstacles or vegetation canopy) and is directly affected by mechanical and buoyancy forcings generated at the surface. It is assumed that in this layer the fluxes are nearly constant with height, and that at a given height reflects a process that is in equilibrium with the upwind surface or "footprint." In this layer, stability effects on wind speed, temperature, and humidity profiles need to be accounted for when using a flux gradient profile technique to estimate fluxes of momentum, heat, and water vapor. In addition, local surface and micrometeorological conditions that contribute to the production of mechanical (wind shear) and buoyancy forces (heat and water vapor) affecting the stability of the surface layer need to be accounted for as well. In general this can be accomplished by computing non-dimensional stability parameters that relate the contribution of buoyancy to those of mechanical forces from the same measurements used to compute turbulent fluxes of momentum, heat, and water vapor.

NON-DIMENSIONAL STABILITY PARAMETERS

In micrometeorology two forms of non-dimensional stability parameters have been developed to characterize diabatic forcings (non-neutral conditions) near the surface. The first was proposed by Richardson (1920) in the form of a

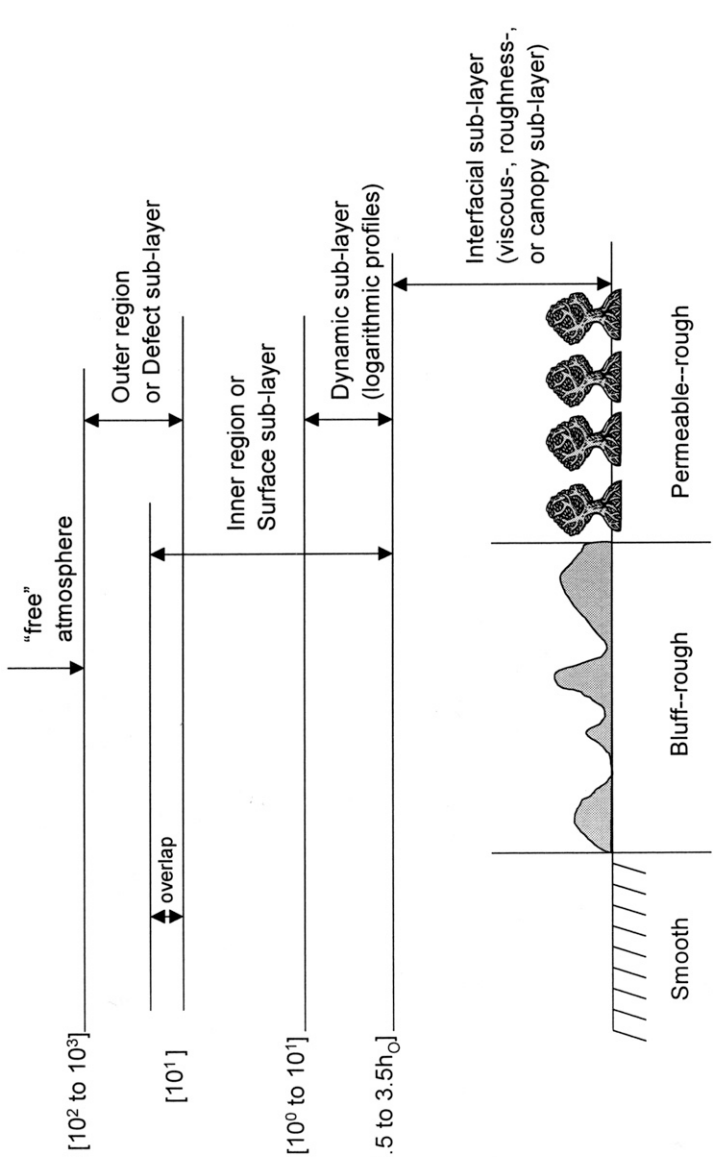

Fig. 18–1. Schematic of the relative depths (in meters) of the sub-layers of the atmospheric boundary layer (ABL); h_o is typical height of the roughness obstacles (Brutsaert, 1982).

ratio that accounts for the effects of buoyancy and mechanical forcings and is expressed as

$$Ri = \frac{g\left(\partial\theta / \partial z\right)}{T_a\left(\partial u / \partial z\right)^2} \quad [7]$$

where g is the acceleration due to gravity (m s^{-2}), $\partial\theta/\partial z$ and $\partial u/\partial z$ are potential temperature and wind speed gradients (°K and m s^{-1}) respectively and T_a is the mean absolute temperature (°K). This expression is well known as the gradient Richardson number, (*Ri)* and can be interpreted to represent a ratio of the contribution of buoyancy (thermal effects) to mechanical (wind shear) forces. Relative magnitudes of *Ri* provide a sense of the strength of the stability/instability. Negative values of *Ri* indicate conditions of instability where surface heating enhances buoyancy effects. These conditions are often associated with warm sunny days. Positive values of *Ri* indicate a stable condition where temperatures near the surface are cooler than away from the surface, a condition that essentially dampens buoyancy forces and ultimately turbulence. Stable conditions are generally associated with early morning, evening–night periods and overcast days. Richardson numbers approaching zero indicates neutral stability generally associated with early morning and/or evening periods on cloudy days with strong winds. Unstable and stable conditions typically will dominate a diurnal cycle with neutral conditions representing a minor fraction of a day.

Monin and Obukhov (1954) proposed a more rigorous theoretical indicator of stability as

$$\varsigma = \frac{z}{L} = \frac{z - d_o}{L} \quad [8]$$

where z is height above a surface (m), d_o is a displacement height (m) associated with vegetated canopies. The stability length scale L (m) is a function of momentum and heat fluxes (Obukhov, 1946) and is expressed in original form as

$$L = -\frac{T_a u_*^3 \rho C_p}{kgH} \quad [9]$$

later modified to include the contribution of buoyancy from evaporation effects (Businger & Yaglom, 1971) to be

$$L = \frac{-u_*^3 \rho}{kg\left[\left(\frac{H}{T_a C_p}\right) + 0.61E\right]} \quad [10]$$

where g, ρ, T_a, and C_p have been previously defined, u_* is friction velocity (m s^{-1}) where qualitatively it can be considered proportional to the tangential rate of rotation of frictionally driven eddies in a flow, k is a constant assumed to be ~0.40, (von Kármán's = u_* $\{z\ \partial u/\partial z\}^{-1}$) H is sensible heat flux (W m^{-2}), and E is

the water vapor or evaporative flux (kg m^{-2} s^{-1}). Because L represents all of the parameters (except height) related to mechanical and buoyancy forces, it is considered a more absolute indicator of stability. Similar to the Ri number, negative values of ζ indicate unstable and positive values represent stable conditions.

It has been assumed in some past investigations that under unstable conditions and very near the surface (~2 m) that $Ri \approx \zeta$. Comparing and evaluating results from recent studies by Dyer and Bradley (1982), Webb (1982), Högström, (1988), and Kader and Yaglom, (1990), Högström, (1996) concluded that the relationship between Ri and ζ was better represented by $Ri \approx 1.5\zeta$. In practice, the Ri number is easier to calculate, since it is computed directly from measurements of temperature and wind speed in a vertical profile configuration above a surface. In contrast, the Monin-Obukhov stability length, while more theoretically robust, requires either more complicated measurements of u_*, H, and E or an iterative scheme using profiles of wind, temperature, and humidity (Brutsaert, 1982); however, ζ does include the buoyancy effects from temperature and humidity (it is embedded in H and E) and thus it is on a practical and theoretical level generally preferred over Ri.

MONIN-OBUKHOV SIMILARITY THEORY

At this point, we introduce the theory of surface layer similarity proposed by Monin and Obukhov (1954). Simply stated, this theory relates surface fluxes of momentum, sensible heat, and water vapor with profiles of wind speed, potential temperature, and humidity in a horizontally homogeneous atmospheric surface layer. For several decades, Monin-Obukhov similarity theory (MOST) has been the approach relating mean profiles of scalars and wind speed to turbulent fluxes of heat, water vapor, and momentum (Brutsaert, 1982; Stull, 1988). Early MOST research efforts were focused on relatively flat, uniform and often well watered vegetated surfaces (agricultural fields) to evaluate turbulent fluxes. In recent years, MOST has been extended to include a class of scalars often referred to as trace gases (CO_2, CH_4, NH_3, and NO_2). Further research progression extended the use of MOST from homogeneous to heterogeneous (sparse or patchy) vegetated surfaces, irregular or sloping terrain. The results of such efforts have been mixed.

Under neutral atmospheric conditions in the lower atmosphere, there exists a relationship between u_* (which is proportional to momentum flux) and the vertical gradient of mean horizontal wind flow. This relationship is expressed as

$$\frac{\partial u}{\partial z} = \frac{u_*}{kz} \qquad [11]$$

where all terms have been previously defined. In a shallow layer above the surface, turbulent fluxes of momentum, heat, water vapor, etc. are approximately constant with height and thus u_* is assumed to be constant with height, although in reality this is not strictly true. Practically, if the change in u_* varies by <10% with height then u_* is considered constant with height. Integrating Eq. [11] from a

height near a surface where u approaches 0 to any height z above a surface results in the expression for the logarithmic wind profile

$$u = \frac{u_*}{k} \ln\left(\frac{z - d_o}{z_{om}}\right) \quad [12]$$

This expression relates the flux of momentum to a wind speed gradient where z_{om} is a scaling parameter (m) that represents the aerodynamic roughness of the surface over which the wind speed profile is measured. The displacement height d_o is referred to as the zero-plane displacement and is considered to represent the mean level at which momentum is absorbed by individual elements of a plant or surface community. Specifically, it is the conceptual level of the effective sink for momentum (Thom, 1971, 1975).

Empirical correlations have suggested that d_o and z_{om} can be reasonably approximated by simple expressions (Allen et al., 1989)

$$d_o = 0.67 h_{vs} \quad [13]$$

$$z_{om} = 0.12 h_{vs} \quad [14]$$

where h_{vs} is the height of a vegetated surface.

Similar relationships also can be derived for sensible heat and water vapor as

$$\frac{\partial \overline{\theta}}{\partial z} = \frac{T_*}{kz} \quad [15]$$

$$\frac{\partial \overline{q}}{\partial z} = \frac{q_*}{kz} \quad [16]$$

where T_* and q_* are scaling parameters defined as

$$T_* = \frac{H}{\rho C_p u_*} \quad [17]$$

$$q_* = \frac{E}{\rho u_*} \quad [18]$$

Equations [11], [15], and [16] are only valid for the neutral stability case, a condition in the natural environment that is not often encountered. Under non-neutral conditions, (strong surface heating or temperature inversions, much more often the case) buoyancy forces will distort the structure and intensity of turbulence and thus the shape of the profiles for momentum, heat, water vapor, etc. In short, unstable conditions enhance upward turbulence motion, distorting the logarithmic profiles and thus affecting the relationships between fluxes and mean gradients, Thom (1975). Stable conditions act to suppress turbulence motion. For the neutral case, only mechanical or friction derived turbulence exists; however, in non-neutral cases, profile distortions need to be accounted for and can be accom-

plished by using empirically derived non-dimensional functions of either *Ri* or ζ. Largely on the basis of a dimensional argument Monin and Obukhov (1954) established flux-profile generalizations to account for non-neutral conditions when computing turbulent fluxes.

Combining Eq. [11], [15], and [16], with Eq. [8] and rearranging with a functional dimensionless expression to account for non-neutral conditions results in the following expressions for momentum, heat, and water vapor;

$$\frac{\partial u}{\partial z}\frac{kz}{u_*} = \phi_m(\zeta) \quad [19]$$

$$-\frac{\partial \theta}{\partial z}\frac{kz}{T_*} = \phi_h(\zeta) \quad [20]$$

$$-\frac{\partial q}{\partial z}\frac{kz}{q_*} = \phi_q(\zeta) \quad [21]$$

where ϕ_m, ϕ_h, and ϕ_q represent "universal" non-dimensional wind, temperature, and water vapor profile functions of ζ (or *Ri*). Equations [19], [20], and [21] are the fundamental expressions in differential form for MOST to relate surface fluxes of momentum, heat, and water vapor to profile gradients.

SURFACE-LAYER STABILITY CORRECTIONS

Equations [19], [20], and [21] contain non-dimensional stability corrections or ϕ functions that are assumed to be "universal." Quotations are used to alert the reader that this is a relative term and is limited to cases where MOST is applicable. Much of the theoretical development and experimental research of the ϕ functions has been focused on the transport of momentum and heat, ϕ_m and ϕ_h, respectively. The number of studies specific to water vapor transport (ϕ_q) is small compared with momentum and heat transport (ϕ_m and ϕ_h). Limited reliable measurements of humidity or water vapor profiles may have contributed to this. For the present we adopt the assumption found in the literature (e.g., Dyer, 1967) of $\phi_h \approx \phi_q$. Simply stated, stability (mechanical and buoyancy) induced transport affects heat, water vapor, and other atmospheric constituents in largely the same way (Crawford, 1965; Dyer, 1967). It is noted, however, that theoretical and experimental work by Warhaft (1976) and Verma et al. (1978), respectively, and comments by Brost (1979) and Hicks and Everett (1979) suggest caution in adhering to the assumption of $\phi_h \approx \phi_q$.

Φ FUNCTION: EARLY SEMI-EMPIRICAL FORMULATIONS

The influence of stability (stable or unstable atmospheric conditions) on the turbulent transport of scalars and momentum near a surface has been a focus of study dating back to the 1940s (Holzman, 1943; Deacon, 1949). Early efforts were directed toward understanding and developing theoretical as well as func-

tional relationships of a non-linear physical process relating the transport of momentum and energy to gradients of wind speed and scalars (temperature and water vapor) Lettau (1949), Deacon (1955), Monin and Obukhov (1954), Kazanski and Monin (1956), Ellison (1957), Swinbank (1960), Panofsky et al. (1960), Panofsky (1961a,b), Sellers (1962).

Various forms of ϕ functions used to account for stability effects began appearing in the early 1960s from several investigators independently. The earliest form was an interpolation function for the known behavior of Eq. [11] under free and forced convection conditions. This expression was derived in different ways independently by Kazanski and Monin (1956), Ellison (1957), Yamamoto (1959), Panofsky (1961a), and Sellers (1962) and was expressed as

$$\phi^4 + \gamma\phi^3\zeta \qquad [22]$$

where γ is a constant, $\phi = (kz/u_*)/(\partial u/\partial z)$, and ζ is defined in Eq. [8]. Equation [22] is in algebraic form expressing a relationship between wind shear (ϕ) and the stability length ζ (z/L) and is recognized as the **KEYPS** function after the names of its originators (**K**azanski & **M**onin, 1956; **E**llison, 1957; **Y**amamoto, 1959; **P**anofsky, 1961a; **S**ellers, 1962). As an interesting note, Businger and Yaglom (1971) point out that Obukhov (1946) proposed the same functional interpolation formula that embraced the entire range of stabilities and thus suggest that a more appropriate name for Eq. [22] perhaps should be **O'KEYPS** since Obukhov (1946) predates the others by nearly a decade.

Equation [22] is a semi-empirical function that had wide use during the sixties (Lumley & Panofsky, 1964). The derivation was fully justified at that time since there were no direct data to determine the experimental form of the relationships. In 1960, Webb (1960) proposed a two-part function for ϕ with continuous first, second, and third derivatives at the junction for the stable and unstable cases. For the stable condition this was expressed as

$$\phi = 1 + 4.5\frac{z - d_o}{L} \qquad [23]$$

and for the unstable condition

$$\phi = 0.316\left(\frac{-(z - d_o)}{L}\right)^{-1/3} - 0.00143\left(\frac{-(z - d_o)}{L}\right)^{-4/3} \qquad [24]$$

Equations [23] and [24] are functional approximations to Eq. [22], which is in fact a differential equation when appropriate substitutions are made. These expressions were valid for the range of $-\zeta \le 0.0317$ for the stable case and $-\zeta > 0.0317$ for the unstable condition. Equations [23] and [24] represent early examples of the empirical functional forms of surface-layer stability corrections for wind profile measurements (Panofsky, 1963).

Since then, numerous forms of ϕ corrections have been derived and/or modified from various studies. Literature citations will be limited to several review articles dealing with this topic (Dyer, 1974; Yamamoto, 1975; Yaglom, 1977; Foken & Skeib, 1983; Högström, 1988; Högström, 1996). Tables 18–1 and

Table 18–1. Examples of functional stability corrections for momentum, heat, and water vapor for the unstable case.

Authors	Comments	Unstable Case for Momentum	Unstable Case for Heat	Unstable Case for Water Vapor
Swinbank, 1964	Exponential wind profile, short annual barley grass	$\phi_m = \zeta[1-\exp(\zeta)]^{-1}$	—	—
Swinbank, 1968	Eddy covariance estimates of H; using $k = 0.40$, short annual barley grass	$\phi_m = [0.613(-\zeta)]^{-1/5}$, $-2 \le \zeta \le -0.1$	$\phi_h = [0.227(-\zeta)]^{-0.44}$, $-2 \le \zeta \le -0.1$	—
Dyer & Hicks, 1970 (as suggested by Businger, 1966)	Profile measurements and eddy covariance estimates of H and u_*, $k = 0.41$, plowed field	$\phi_m = [1-16(\zeta)]^{-1/4}$, $-1 \le \zeta \le -0.1$	$\phi_h = [1-16(\zeta)]^{-1/2}$, $-1 \le \zeta \le -0.1$	$\phi_q = [1-16(\zeta)]^{-1/2}$, $-1 \le \zeta \le -0.1$
Webb, 1970	Using profiles only, no comparison with eddy covariance fluxes, short grass	$\phi_m = 1+4.5(\zeta)$, $\zeta < -0.03$	$\phi_h = 1+4.5(\zeta)$, $\zeta < -0.03$	$\phi_q = 1+4.5(\zeta)$, $\zeta < -0.03$
Businger et al., 1971	Using $k = 0.35$ and eddy covariance estimates of fluxes, wheat stubble	$\phi_m = [1-15(\zeta)]^{-1/4}$, $-2 \le \zeta \le 1.25$	$\phi_h = [0.74(1-9(\zeta))]^{-1/2}$, $-2 \le \zeta \le 1.25$	—
Pruitt et al., 1973	Profile measurements, drag plate measurements for J, weighing lysimeter for E, $k = 0.42$, turf grass	$\phi_m = (1-16Ri)^{-1/3}$, $-3.5 \le Ri \le 0$	—	$\phi_w = [0.885(1-22Ri)]^{-2/5}$, $-3.5 \le Ri \le 0$
Dyer & Bradley, 1982	$k = 0.40$, burnt grass	$\phi_m = [1-28(\zeta)]^{-1/4}$, $\zeta \ge -2$	$\phi_h = [1-14(\zeta)]^{-1/2}$, $\zeta \le 0$	—
Foken & Skeib, 1983	$k = 0.40$, Russian steppes	$\phi_m = 1$, $-2 \le \zeta \le -0.06$ $\phi_m = (-\zeta / 0.06)^{-0.25}$, $\zeta \le -0.06$	$\phi_h = 1, \zeta > -0.06$ $\phi_h = (\zeta / 0.06)^{-0.5}$, $\zeta \le -0.06$	—
Högström, 1996	$k = 0.40$, data representing multiple surfaces from oceans to forests	$\phi_m = (1-19(\zeta)^{-1/4}$, $\zeta \le -2$	$\phi_h = [0.95(1-11.6(\zeta)]^{-1/2}$, $-\zeta \le 2$	—

Table 18–2. Examples of functional stability corrections for momentum, heat, and water vapor for the stable case.

Authors	Comments	Stable Case for Momentum	Stable Case for Heat	Stable Case for Water Vapor
Webb, 1970	Using profiles only, no comparison with eddy covariance fluxes, short grass	$\phi_m = (1+5.2\zeta)$, $-0.03 \le \zeta \le 1$	$\phi_h = (1+5.2\zeta)$, $-0.03 \le \zeta \le 1$	$\phi_q = (1+5.2\zeta)$, $-0.03 \le \zeta \le 1$
Businger et al., 1971	Using $k = 0.35$ and eddy covariance estimates of fluxes, wheat stubble	$\phi_m = (1+4.7\zeta)$, $-2 \le \zeta \le 1$	$\phi_h = (0.74+4.7\zeta)$, $-2 \le \zeta \le 1$	—
Pruitt et al., 1973	Profile measurements, drag plate measurements for J, weighing lysimeter for E, turf grass	$\phi_m = (1+16Ri)^{1/3}$, $0 \le Ri \le 0.3$	—	$\phi_w = [0.885(1+34Ri)]^{2/5}$, $0 \le Ri \le 0.3$
Dyer, 1974	Profile measurements and eddy covariance estimates of H and u_*, $k = 0.41$,	$\phi_m = 1+5(\zeta)$, $0 \ge \zeta \ge -1$	$\phi_h = 1+5(\zeta)$, $0 \ge \zeta \ge -1$	$\phi_q = 1+5(\zeta)$, $0 \ge \zeta \ge -1$
Dyer & Bradley, 1982	$k = 0.41$, burnt grass	$\phi_m = (1-28(\zeta)^{-1/4}$, $\zeta \ge -2$	$\phi_h = (1-14(\zeta)^{-1/2}$, $\zeta \ge -2$	—
Foken & Skeib, 1983	$k = 0.40$, Russian steppes	$\phi_m = 1, \zeta \ge -0.06$ $\phi_m = (\zeta / 0.06)^{-1/4}$, $\zeta \le -0.06$	$\phi_h = 1, \zeta \ge -0.06$ $\phi_h = (\zeta / 0.06)^{-1/2}$, $\zeta \le -0.06$	—
Högström, 1996	$k = 0.40$, data representing multiple surfaces from oceans to forests	$\phi_m = 1+5.3(\zeta)$, $0 \le \zeta \le 0.5$	$\phi_h = 1+8.0(\zeta)$, $0 \le \zeta \le 0.5$	—

18–2, however, will contain examples of stability corrections from many other investigators for both stable and unstable cases across a variety of surfaces. This list will enable the reader to quickly review important contributions to this topic spanning the last 30 years.

UNSTABLE CASE

Dyer and Hicks (1970) provide one of the more recognized and used forms of the universal functions for the unstable case for momentum and heat transport

$$\phi_m = (1 - 16\zeta)^{-1/4} \quad [25]$$

$$\phi_h = (1 - 16\zeta)^{-1/2} \quad [26]$$

where, subscripts m and h refer to momentum and sensible heat fluxes, respectively. These forms were derived on the assumption that von Kármán's constant is equal to 0.41. The range of ζ is $-1 \leq \zeta \leq 0$, where negative ζ represents unstable conditions associated with daytime surface heating. It is noted again that near the surface (approximately 2 to 3 m above) the gradient Richardson number (Ri) has been used in place of ζ. Businger (1987) provides supporting data on the appropriateness of this assumption. The following year Businger et al. (1971) reported similar ϕ functions for the unstable case as

$$\phi_m = (1 - 15\zeta)^{-1/4} \quad [27]$$

$$\phi_h = 0.74(1 - 9\zeta)^{-1/2} \quad [28]$$

where ζ includes the range $-2 \leq \zeta \leq 1$. Equations [25], [26], [27], and [28] have been widely used and are found in most textbooks related to micrometeorology. It has been suggested that the difference in the value of the von Kármán's constant (0.41 for Dyer and Hicks, 1970, compared with 0.35 for Businger et al., 1971) may have contributed to the differences. Literature values for the von Kármán constant range from 0.35 to 0.43 and remains somewhat an unresolved issue, however, most studies use $k = 0.40$. Note that for the momentum case, Eq. [25] and [27] are nearly identical differing only slightly in the value of the constant (15 compared with 16).

For sensible heat, in addition to the incorporation of Prandtl's number (0.74), a considerable difference between the constants for Eq. [24] and [26] is observed. The range for ζ is greater for the Businger et al. (1971) corrections than for Dyer and Hicks (1970) by a factor of nearly two suggesting applicability across a wider range of atmospheric surface conditions. Pruitt et al. (1973) reported ϕ corrections for momentum and water vapor profiles over turf grass (*Poaceae* sp.) as

$$\phi_m = (1 - 16Ri)^{-1/3} \quad [29]$$

$$\phi_q = [0.885(1 - 22Ri)]^{-2/5} \quad [30]$$

In that study, measurements of evaporation and momentum were made using a precision weighing lysimeter (for evaporation) and a floating drag-plate lysimeter (for momentum). This study was unique since water vapor was considered. Note the use of Ri in place of ζ ($Ri \cong \zeta$). The results represented an even wider range of stabilities ($-3.5 \leq Ri \leq 0$) than those of Businger et al. (1971).

Equations [25], [26], [27], [28], [29], and [30] represent important contributions from a period (1970–1973) in which theoretical flux-gradient relationships were fitted with results from field experiments for the unstable case. Profile estimates were compared with measurements of evaporation and sensible heat fluxes from eddy covariance or lysimeters. As a result, eddy fluxes and vertical profiles were independently determined and then related within the Monin-Obukhov framework. Prior to the work of Dyer and Hicks (1970) and Businger et al. (1971), there were few direct data permitting one to determine the experimental form of these relationships with Swinbank (1964, 1968) being the exception.

STABLE CASE

Considering now the stable case, Webb (1970), Businger et al. (1971), and Pruitt et al. (1973) provide early expressions that are frequently cited in which under stable conditions the effects on momentum, heat, and water vapor transport are assumed to be more or less equivalent.

From Webb (1970) the correction is simply expressed as,

$$\phi_m = \phi_h = \phi_q = 1 + 5.2\zeta \quad [31]$$

while Businger et al. (1971) expressed momentum and heat flux corrections as

$$\phi_m = 1 + 4.7\zeta \quad [32]$$

$$\phi_h = 0.74 + 4.7\zeta \quad [33]$$

and from Pruitt et al. (1973) for momentum and water vapor,

$$\phi_m = (1 + 16Ri)^{1/3} \quad [34]$$

$$\phi_q = 0.885(1 + 34Ri)^{2/5} \quad [35]$$

The variability among the ϕ expressions for the stable case is striking (see Tables 18–1 and 18–2) suggesting difficulties in the MOST approach that have yet to be resolved and raising questions about the limitations and under what conditions MOST becomes tenuous. It has been suggested that perhaps this may be related to sources of errors arising from instrument calibration–measurement technique (Yaglom, 1977). While this always remains a possibility with past, present and future studies, it may not necessarily have anything to do with instrumentation. It is important to recognize the random statistical variability of atmospheric behavior. The assumption of surface layer atmospheric stationarity can often be vio-

lated by meso-scale events intermittently imposed on any given study site. These can include wind speed, radiation and wind direction that can in turn cause surface fluxes of momentum, sensible, and latent heat to be highly variable so that ultimately a given flux-gradient averaging period will be affected.

SUMMARY OF THE GRADIENT STABILITY FUNCTIONS

It should be emphasized that while the constants for the various ϕ functions have varied from study to study, some more appreciably than others, the general form of the equations for unstable and stable conditions remains largely the same. For the unstable case involving momentum, heat, and water vapor transport this can be expressed in general form as

$$\phi_i = (1 - \beta\zeta)^{-\alpha} \quad [36]$$

where values of β can range from 0.227 to 28 and α between 0.2 and 0.5 (Table 18–1). Expanding Eq. [36] to represent specific generalized forms as proposed by Businger, (1966) and Dyer and Hicks, (1970) one arrives at

$$\phi_m = (1 - \gamma\zeta)^{-1/4} \quad [37]$$

$$\phi_h = (1 - \gamma\zeta)^{-1/2} \quad [38]$$

$$\phi_q = (1 - \gamma\zeta)^{-1/2} \quad [39]$$

where γ in this case is equal to 16. Additionally Businger (1966) and Pandolfo (1966) suggested that there is no distinguishable difference between ϕ_h and ϕ_q in the unstable case and that each can be well described by the square of ϕ_m and suggested a more general expression as

$$\phi_m^{\,2} = \phi_h = \phi_q = (1 - 16\zeta)^{-1/2} \quad [40]$$

The generalized form for the stable condition (Webb, 1970) can be expressed as

$$\phi_m = \phi_h = \phi_q = 1 + 5\zeta \quad [41]$$

INTEGRATED FORMS OF THE FLUX-GRADIENT AND STABILITY FUNCTIONS

Equations [19], [20], and [21] represent differential functional expressions for the transfer of momentum, heat, and water vapor. When making profile measurements of wind speed, temperature, and humidity, one is actually measuring the difference (Δu, ΔT, and Δq) between any two or more heights and not the derivative (∂u, $\partial\theta$, and ∂q). The stability correction functions summarized in Tables 18–1 and 18–2 are functional forms for the derivative expressions for momentum heat and water vapor. To appropriately use the stability corrections

with actual measurements, an integration needs to be performed with respect to z from $z = d_o + z_{om}$, where $u = 0$ according to Eq. [11] to an appropriate height in the surface sub-layer.

The relationships between surface fluxes (momentum, sensible heat, and evaporation) and measured mean wind speed, temperature, and water vapor profiles from a profile configuration above the roughness sub-layer can now be expressed respectively as finite differences. These forms allow for direct implementation of measured profiles of wind speed, temperature and humidity over a surface and are expressed as

$$\Delta\overline{u} = \overline{u}_2 - \overline{u}_1 = \frac{u_*}{k}\left[\ln\left(\frac{\zeta_2}{\zeta_1}\right) - \psi_m\left(\zeta_2\right) + \psi_m\left(\zeta_1\right)\right] \quad [42]$$

$$\Delta\overline{\theta} = \overline{\theta}_1 - \overline{\theta}_2 = \frac{H}{ku_*\rho C_p}\left[\ln\left(\frac{\zeta_2}{\zeta_1}\right) - \psi_h\left(\zeta_2\right) + \psi_h\left(\zeta_1\right)\right] \quad [43]$$

$$\Delta\overline{q} = \overline{q}_1 - \overline{q}_2 = \frac{E}{ku_*\rho}\left[\ln\left(\frac{\zeta_2}{\zeta_1}\right) - \psi_q\left(\zeta_2\right) + \psi_q\left(\zeta_1\right)\right] \quad [44]$$

where all terms have been previously defined. Here, ψ_m, ψ_h, and ψ_q are the integrated forms for the respective stability corrections and subscripts 1 and 2 refer to arbitrary measurement heights above a surface. Equations [42], [43], and [44] represent extensions of the logarithmic profiles to non-neutral conditions where ψ_m, ψ_h, and ψ_q are stability functions for momentum, heat, and humidity now defined in general integral form similar to Panofsky (1963) as

$$\psi_m = \int_{\left(z_{om}/L\right)}^{\xi}\left[1 - \phi_m\left(\xi\right)\right]d\xi / \xi \quad [45]$$

$$\psi_h = \int_{\left(z_{oh}/L\right)}^{\xi}\left[1 - \phi_h\left(\xi\right)\right]d\xi / \xi \quad [46]$$

$$\psi_q = \int_{\left(z_{oq}/L\right)}^{\xi}\left[1 - \phi_q\left(\xi\right)\right]d\xi / \xi \quad [47]$$

The general ϕ (Eq. [37] [38], and [39]) can now be integrated with Eq. [45], [46], and [47]. Roughness lengths of z_{oi} (where i represents m, h, and q) for momentum, heat, and humidity, respectively, are generally significantly smaller than L, and thus in this example the lower limit of the integral is assumed to be zero (Paulson, 1970) resulting in the following profile functions for the unstable case ($\zeta < 0$)

$$\psi_m = 2\ln\left(\frac{1+\xi}{2}\right) + \ln\left(\frac{1+\xi^2}{2}\right) - 2\arctan\left(\xi\right) + \frac{\pi}{2} \quad [48]$$

$$\psi_h = 2\ln\left(\frac{1+\xi^2}{2}\right) \quad [49]$$

$$\psi_q = 2\ln\left(\frac{1+\xi^2}{2}\right) \quad [50]$$

where in this example assuming equality of the ϕ functions for momentum, heat, nd humidity, express ξ as (Brutsaert, 1982)

$$\xi = (1 - 16\zeta)^{-1/2} \quad [51]$$

For the stable case less is known about the flux-profile relationships compared with the unstable case. Early on there was optimism that the log-linear functions would have applicability across a range encompassing both stable and unstable conditions. As can be observed in Tables 18–1 and 18–2 variations in the range of ζ by independent investigators suggest limited applicability for different functions. There is, however, general consensus that log linear profiles may be suitable for moderately stable conditions (McVeil, 1964; Webb, 1970; Businger et al., 1971); however, for strongly stable conditions ($\zeta > 1$) variability of the values of the parameters continue to persist. For practical flux computation under stable conditions the exact analytical form of the ϕ functions is not critical. This is largely due to the fact that under stable conditions turbulent fluxes of mass and energy tend to be rather small and thus use of Eq. [41] (Webb, 1970) is generally considered acceptable. Equations [42], [43], and [44 are now in analytical form to be used with carefully measured wind speed, temperature, and humidity profiles to compute fluxes of momentum and heat.

FLUX-GRADIENT-MOST APPROACH WITH SURFACE BOUNDARY CONDITIONS

An alternative flux-gradient application involves the use of surface boundary conditions. Assuming surface boundary conditions of $u = 0$ at $z = d_o + z_{om}$ and an observation of surface temperature, θ_S (typically measured with an infra-red sensor), only one level (as opposed to two) of u, θ, and q measurements are required so that the equations have the following forms:

$$u_z - u_s = u_*/k\{\ln[\_z - d_o)/z_o] - \psi_m[(z - d_o)/L]\} \quad [52]$$

$$\theta_s - \theta_z = T_*/k\{\ln[z - d_o)/z_{oh}] - \psi_h[(z - d_o)/L]\} \quad [53]$$

$$q_s - q_z = q_*/k\{\ln[\_z - d_o)/z_{oq}] - \psi_q[(z - d_o)/L]\} \quad [54]$$

where the subscript s denotes measured parameters at the surface. Specifically, $q_s = q^*(\theta_S)\, RH_S$ where RH_S is surface humidity and $q^*_S(\theta_S)$ is the saturated specific humidity at a surface temperature θ_S. Equations [52], [53], and [54] also have

been called bulk-transfer formulations (Brutsaert, 1982). These equations require estimates of surface roughness for momentum, (z_{om}) heat, (z_{oh}) and water vapor (z_{ov}) as well as an estimate of RH_S, which is not easily measured thus limiting the practical use of Eq. [54].

In the context of Monin-Obukhov surface layer similarity theory, both theory and field observations indicate that transfer of momentum is more efficient than for heat (Brutsaert, 1982). This transfer process is characterized by parameterizing different roughness lengths for momentum, heat, and water vapor. Physically this means that over rough surfaces, transfer mechanisms for momentum are a function of shear forces created by the interaction of momentum with the individual roughness elements. Depending on size, density, and distribution of the roughness elements, local pressure gradients also may be generated as a result of interactions of momentum with individual roughness elements creating an effective form drag at the surface. In contrast to scalar admixtures (e.g., temperature, water vapor, trace gases), the transfer processes are primarily controlled by molecular diffusion. Thus a large range in the magnitude for the different roughness lengths can be expected. All, however, represent a length scale that can be generally interpreted to represent the relative transport efficiency of scalars and momentum as it relates to surface roughness and degree of heterogeneity.

For homogeneous surfaces the ratio of roughness lengths for momentum, z_{om}, and heat, z_{oh}, is essentially a constant, usually expressed as the natural logarithm ln (z_{om}/z_{oh}) = kB^{-1} where $kB^{-1} \approx 2$. A distinction is made between surfaces considered bluff-rough (e.g., hilly terrain, urban centers) and permeable-rough (e.g., vegetation) surfaces. For bluff-rough surfaces, the value of kB^{-1} varies from ~1 to ~20 as a function of the momentum scalar roughness Re^* (= $u_* z_{om}/\upsilon$) where u_* is the friction velocity and υ is the kinematic molecular viscosity (Brutsaert, 1982).

Many studies, particularly over partial canopy surfaces, report values of kB^{-1} significantly >2 with the range generally between permeable-rough, $kB^{-1} \approx 2$, and bluff-rough, $kB^{-1} \approx 10$, (Verhoef et al., 1997). Contributing factors include effects of the soil–substrate on remotely sensed surface temperature observations (θ_S), canopy architecture, amount and type of vegetation (McNaughton & Van den Hurk, 1995). Unfortunately, this is a diagnostic tool and is not useful for quantifying evaporation since approaches using radiometric temperature with a single roughness parameter z_{oh} to describe the surface (i.e., single-source approach) are in general unreliable (Verhoef et al., 1997). In fact, in some cases where the soil–substrate is cooler than the canopy, unrealistic negative values of kB^{-1} can be obtained (Sun & Mahrt, 1995). In general, determining appropriate values of roughness parameters for specific surface types remains challenging because no general solution exists for determining z_{oh} and z_{ov}.

More reliable "two-source" approaches are being developed that explicitly compute soil and vegetation heat flux exchanges with the overlying atmosphere and account for component temperature contributions to composite surface temperature observations (Norman et al., 1995). A recent version of the two-source modeling approach has been developed and tested that can be used with continuous θ_S observations for estimating sensible heat fluxes. Minimal inputs of wind speed, air temperature, and solar radiation measurements are required in addition to canopy height, leaf width, and fractional cover (Norman et al., 2000).

It was previously mentioned that application of Eq. [53] is tenuous for most surfaces, in particular for heterogeneous surfaces since z_{oh} has little physical meaning when used with θ_s observations. There has been more progress in relating z_{om} to physical properties of the surface (e.g., Brutsaert, 1982). A unifying approach proposed by Raupach (1992, 1994, 1995) is based on the analytical treatment of drag and drag partitioning for estimating z_{om} requiring appropriate obstacle height and density estimates. When applying Eq. [52] to heterogeneous surfaces, the height of u_z becomes critical since z_{om} reflects the upwind roughness characteristic as a length scale (100 z)where z represents mean obstacle height in m. Tower data have shown that for heterogeneous surfaces, a different z_{om} is required depending on the level(s) of u_z (e.g., Beljaars, 1982). This led to the development of a blending height concept (Wieringa, 1986) and theories for estimating effective roughness; however, recent work indicates existing approaches are not yet satisfactory (Schmid & Bunzli, 1995). Therefore, unless the surface has relatively uniform obstacle height and density at length scales applicable to MOST, the roughness parameters remain ill defined.

LIMITATIONS OF THE FLUX-GRADIENT APPROACH USING MOST

Basic Assumptions

An important point to be considered involves a basic assumption associated with MOST. All measured parameters are in terms of mean values or (appropriate time averages). A critical assumption is that the measurements are conducted under steady state conditions of wind speed and direction. In other words enough eddies in full equilibrium with the underlying surface must advect past the instruments to provide an ensemble average that is representative of the source or footprint. The measurements must be made in the fully adjusted layer and above the roughness sub-layer. This requires sufficiently large homogeneous areas for an adequately equilibrated layer of air to develop and maintain equilibrium during the measurement period. Note that this is an idealized situation not easily accomplished. More typical are cases where the fully adjusted layer may have intermittently superimposed events of instability originating outside the local footprint of the measured profiles. Under this condition, information outside the intended footprint of the measured parameters may be received from elsewhere in the form of large (low frequency) intermittent eddies. This can significantly distort the measured profiles and thus consequently affect computed surface fluxes. Flux-gradient relationships are subject to limitations of any approach that contains a great deal of empiricism.

Stability Correction Functions

When observing the various forms of stability corrections presented in Tables 18–1 and 18–2 it is apparent that the variability of the constants has implications regarding the “universal” application of these forms of stability corrections. More recently, Brutsaert (1992) derived new functional forms for Ψ_m and

Ψ_h based on similarity relationships from Kader and Yaglom (1990). Differences with the classical Businger-Dyer formulations (Dyer, 1974; Businger, 1987) are minor for Ψ_h and thus conceivably for Ψ_q, however, experimental data suggest that under highly unstable conditions (i.e., $(z - d_o)/L$ or $\zeta < -100$) the minor differences in the Businger-Dyer and Kader-Yaglom formulations for Ψ_h can result in significant differences for computed H (Sugita et al., 1995; Kondo & Ishida, 1997). For Ψ_m, the new function of ζ reaches a maximum value on the order of 2 for $\zeta \sim -10$ instead of a monotonically increasing Ψ_m with ζ reaching a maximum on the order of 5 for $\zeta \sim -100$. Moreover, the data scatter observed in many of these studies has not been appreciably reduced during the last three decades despite improved instrumentation and data acquisition systems now readily and economically available.

Early in the development of stability correction functions, Yaglom (1977) suggested several sources of errors contributing to the discrepancies in the functional forms of the stability functions. The first obvious reason may be related to instrument error. Too often, it appears that the role of instrument error is underestimated in the literature as it rarely is even mentioned much less discussed. Often it is assumed that random instrument errors are already accounted for. Intercomparison of instruments needs to be conducted to assess the level of bias of each anemometer, psychrometer, and when possible eddy covariance instrumentation. Quantifying measurement error should be as important as the actual field experiment measurements. Yaglom (1977) provides several examples of what can happen when instrument errors are not appropriately taken into account. Another issue deals with the accuracy of mean temperature, wind and humidity measurements. Although sensors can be matched by inter-calibration before deployment in the field, there are also errors associated with whether or not the temperature–humidity sensors are aspirated and wind sensors (cup anemometers) starting thresholds are similar and how uniformly non-horizontal winds affect the anemometers with height. These issues were recently addressed by Brotzge and Crawford (2000) who attempted to use temperature and wind speed observations at two levels (2 and 10 m AGL) from the Oklahoma Mesonet network to compute sensible heat fluxes via Eq. [6] and [7]. Comparisons with eddy covariance measurements indicated that discrepancies on the order of 100 W m^{-2} during the mid-day period were likely for the 2 m height with wind speeds <4 m s^{-1} while at higher wind speeds the discrepancies were reduced to a range of 50 to 100 W m^{-2}. This was primarily due to a reduction of radiation-induced errors for the non-aspirated temperature sensors. With mid-day H estimates of 200 to 300 W m^{-2}, the magnitudes of the uncertainties may become unacceptable.

Continual modification of stability functions suggests caution in assuming the "universality" of any stability function when applying gradient type approaches for estimating fluxes. Large Eddy Simulation (LES) model analysis of MOST suggests that boundary layer depth has an indirect influence on MOST scaling for wind (Khanna & Brasseur, 1997). Williams and Hacker (1993) analyzed turbulence measurements from an aircraft and showed that mixed-layer convective processes influence MOST and support the refinements made by Kader and Yaglom (1990). Tsvang et al. (1998) suggested that small-scale inhomogeneities of the land surface could cause stability functions to depart signifi-

cantly from predicted values. Clearly considerable uncertainties remain as surface heterogeneity and mixed-layer convective processes can affect "idealized" MOST profiles.

Roughness Sub-Layer Effects

Assuming measurement issues are adequately addressed, there exists the potential problem of roughness sub-layer effects (e.g., Garratt, 1978, 1980) when applying MOST "near" (<3 h_{vs}) a canopy surface. The primary effect of the roughness sub-layer is the production of smaller gradients necessitating larger eddy diffusivities. The depth of the roughness sub-layer, z_R, has been related to surface properties that include momentum roughness length, z_{om}, (Tennekes, 1973), obstacle or vegetation height, h_{vs}, spacing, D_{vs}, (Garratt, 1980) and roughness element lateral dimension (Raupach et al., 1980). Approaches thus far to "correct" flux-profile relationships for roughness sub-layer effects have been semi-empirical, and tend to be surface specific (Garratt, 1980; Raupach et al., 1980; Cellier & Brunet, 1992).

Complicating the roughness sub-layer effect on MOST is that scalar eddy diffusivity enhancement is larger than that for momentum (Thom, 1975; Raupach, 1979; Chen & Schwerdtfeger, 1989). Moreover, Chen and Schwerdtfeger (1989) found that the enhancement was stability dependent and that variations were not monotonic with height. Their review of previous studies on roughness sub-layer effects suggests that $z_R - d_o \sim 4\ D_{vs}$. Use of obstacle spacing appears to give more consistent results with a nearly constant coefficient of proportionality. Relating z_R to other surface parameters leads to larger variations in the coefficient such as z_{om} where, $z_R - d_o \sim 50 - 100\ z_{om}$ as suggested by Tennekes (1973) or in terms of h_{vs} in which case $z_R - d_o \sim 2 - 10\ h_{vs}$. This is due to the effects of obstacle density, height, and structure on turbulent momentum transport (Raupach et al., 1991). Raupach (1994) proposed a relatively simple approach based on roughness density which yields $z_R \sim 2\ (h_{vs} - d_o)$. This later expression, however, does not reproduce the larger values of 5 to 10 h_{vs} observed by Garratt (1980) and Chen and Schwerdtfeger (1989). In addition, the results from Chen and Schwerdtfeger (1989) suggest that a simple expression for estimating z_R for scalars is not yet available. Chen and Schwerdtfeger (1989), Raupach et al. (1991), and Cellier and Brunet (1992) provide an interesting review on mechanisms that enhance eddy diffusivities. Chen (1990a,b) evaluated instantaneous wind and temperature profiles with eddy covariance measurements and found that over brush land, mechanisms for momentum and heat transport are distinct and that large intermittent turbulent structures in the boundary layer can penetrate and modify the fully adjusted layer resulting in significantly distorted profile shapes.

Variance Approach

With the inherent limitations described above in using the flux-gradient-MOST approach as a micrometeorological technique for flux estimation, others have explored the application of MOST with 2nd order turbulent statistics or

variance for wind, temperature, and humidity measurements. Similar to mean profiles of wind, temperature, and specific humidity, the standard deviation of vertical velocity, σ_w, temperature σ_q, and specific humidity σ_q have been related to fluxes via MOST (Panofsky & Dutton, 1984). For unstable conditions,

$$\sigma_w/u_* = c_1[1 - c_2(z - d_o)/L]^{1/3} \quad [55]$$

$$\sigma_\theta/T_* = c_3[c_4 - (z - d_o)/L]^{-1/3} \quad [56]$$

$$\sigma_q/Q_* = c_5[c_6 - (z - d_o)/L]^{-1/3} \quad [57]$$

where the coefficients (c_n, n = 1,2...6) in Eq. [55], [56], and [57] are empirically determined. Strictly speaking, MOST would imply that for scalars, $c_3 \approx c_5$ and $c_4 \approx c_6$. A simplified relationship for σ_θ/T_* derived by Wyngaard et al. (1971) is supported by observations (e.g., Kader & Yaglom, 1990) and expressed as

$$\sigma_\theta/T_* = c_3[(z - d_o)/L]^{-1/3} \quad [58]$$

Substitution of Eq. [9] for L (neglecting the buoyancy effect of water vapor) into Eq. [58] yields an expression that is no longer a function of u_* resulting in H related only to σ_θ,

$$H = \rho C_p \left(\frac{\sigma_\theta}{c_3}\right)^{3/2} \left(\frac{kg\left(z - d_o\right)}{T_A}\right)^{1/2} \quad [59]$$

Similarly LE is related to σ_q and σ_θ,

$$LE = \sigma_q \left(\frac{\sigma_\theta kg\left(z - d_o\right)}{c_3^3 T_A}\right)^{1/2} \quad [60]$$

The magnitudes of the coefficients in Eq. [55], [56], [57], [58], [59], and [60] are on the order of $c_1 \sim 1.25$, $c_2 \sim 3$, $c_3 \sim 0.95$, $c_4 \sim 0.05$, Katul et al. (1995, 1996). Studies over non-uniform surfaces suggest that for water vapor Eq. [57] may not be valid or at the very least the coefficients in Eq. [57] c_5 and c_6 are not equal to c_3 and c_4 and moreover are not constant (see e.g., Katul et al., 1995, 1996). Indications are that for water vapor, several factors may be contributing to Eq. [57], [58], [59], and [60] that result in significant deviation from MOST (Katul et al., 1995): (i) temperature is not a passive scalar but has an active role in enhancing turbulence in the surface layer, (ii) for partially vegetated surfaces the sources and sinks of latent and sensible heat are from significantly different heights–locations, and (iii) the spatial variability of water vapor sources appears to have a more significant impact on MOST relationships than variability of sensible heat sources. Recently, Katul and Hsieh (1999) show analytically through second-order closure principles applied to the flux-budget equations for heat and water vapor that the coefficients c_5 and c_6 are not equal to c_3 and c_4, respectively, even when flux-profile similarity functions for heat and water vapor profile are nearly equal, namely $\phi_H \approx \phi_E$.

Flux-Gradient versus Variance Approach

Examples comparing two aerodynamic methods, flux-gradient–profile and variance technique, applied to measurements made over a heterogeneous desert environment are illustrated in Fig. 18–2 to 18–4. A 10-m tower with wind and temperature profile measurements at 3, 4, 5, 6, 8, and 10 m, along with eddy covariance measurements, which include temperature variance, at 5 m were used in the two approaches (Kustas et al., 1998). These measurements were made over a coppice mesquite dune site at the Jornada Experimental Range near Las Cruces, NM, as part of the JORNEX (JORNada Experiment) project (Havstad et al., 2000).

Computing *H* and *LE* fluxes using gradients near the surface (at 4 and 5 m) and over the entire measurement height (3 and 10 m), the comparison with eddy covariance measurements of sensible heat flux, *H*, shows significant bias (Fig.

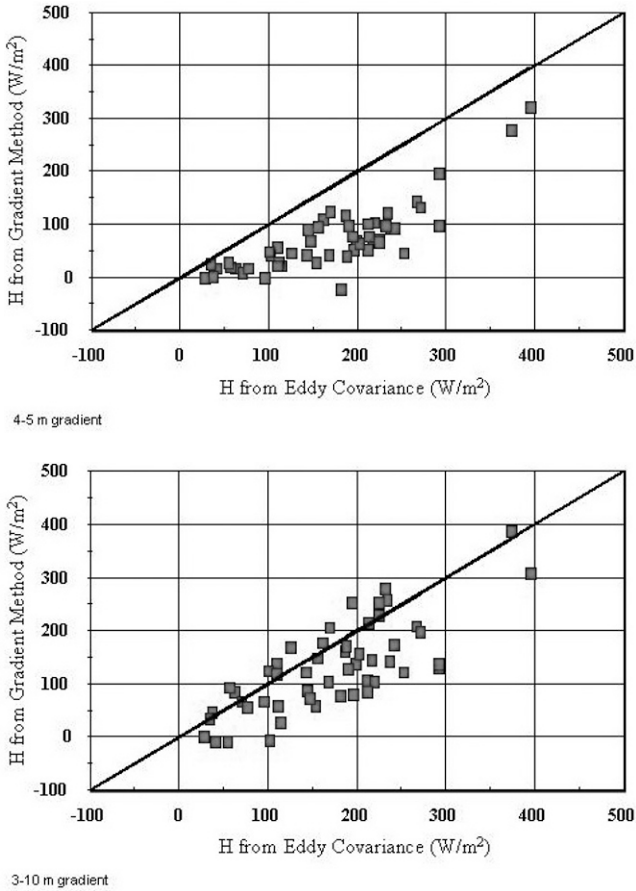

Fig. 18–2. Comparison of flux-gradient approach applied near the surface (a) (4–5 m gradient) (b) 3–10 m gradient) vs. eddy covariance measurement of sensible heat flux, *H*, over a coppice dune site.

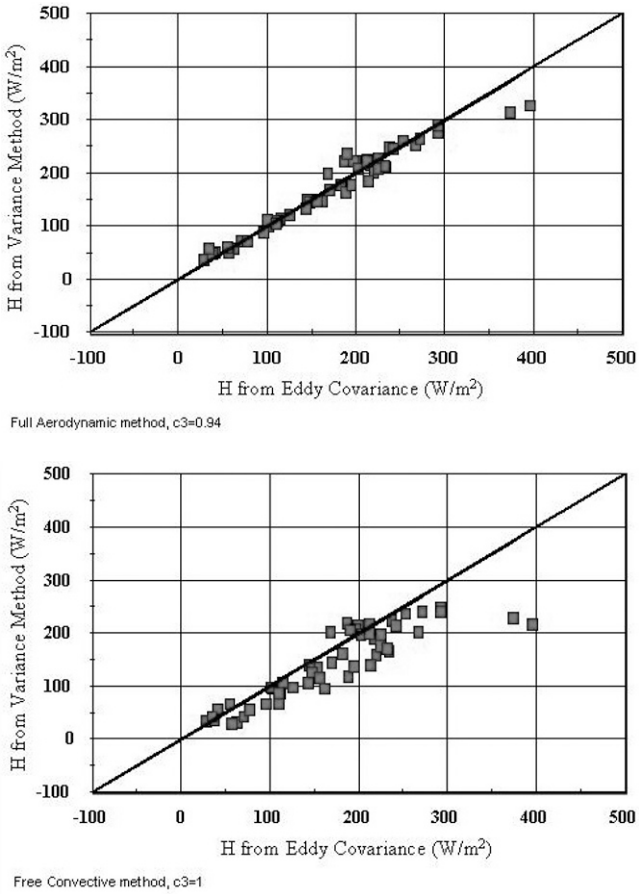

Fig. 18–3. Comparison of variance technique using (a) Eq. [50] and [51] (full aerodynamic method) with $c_3 = 0.94$ and (b) using Eq. [54] (free convective limit with a global value for c_3 (i.e., $c_3 = 1$) for estimating sensible heat flux, H, versus eddy covariance measurements over a coppice dune site.

18–2a) as well as scatter (Fig. 18–2b). The bias in the application of the flux-gradient method near the surface (Fig. 18–2a) is most likely caused by roughness sub-layer effects discussed previously. The scatter observed in Fig. 18–2b may be due to several factors, including roughness sub-layer effects, the uncertainty in the measurement of the gradients, and the MOST stability functions. In both applications using MOST with the mean profile measurements, there is generally poor performance in the estimation of sensible heat flux. The root-mean-square-error (RMSE) with the H observations is ~110 W m^{-2} and ~70 W m^{-2} using MOST flux-profile approach with 4 to 5 m, and 3 to 10 m gradients. Similar RMSE values were obtained by implementing flux-gradient methods using the Oklahoma Mesonet data collected over much more uniform vegetated grassland areas (Brotzge, 2000, personal communication).

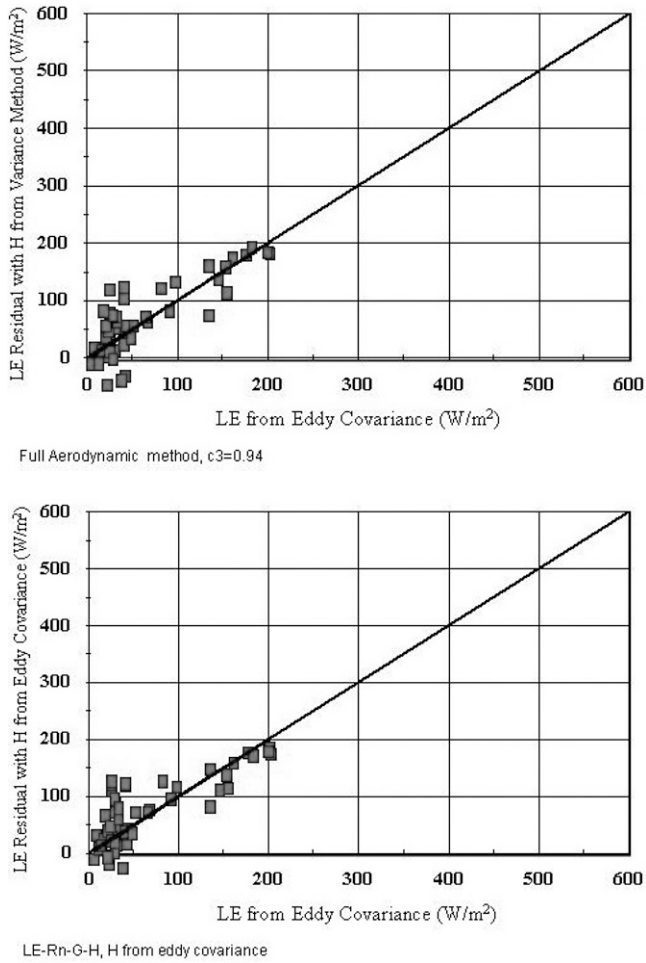

Fig. 18–4. Comparison of latent heat flux, *LE*, solved by residual using measurements of *Rn*, *G*, and *H* (a) estimated by the variance technique (Eq. [50] and [51]) (b) measured by eddy covariance versus *LE* from eddy covariance.

Using the variance method, the agreement with the sensible heat flux observations is significantly improved (Fig. 18–3). This is particularly true when applying the full aerodynamic formulation involving Eq. [50] and [51] with coefficient c_3 calibrated for the particular site (Fig. 18–3a); however, even applying the free convective limit (Eq. [54]) with a "global" value for c_3 (i.e., $c_3 = 1$), the method yields acceptable *H* estimates (Fig. 18–3b). The RMSE with the *H* observations is ~20 W m^{-2} and ~45 W m^{-2} using two versions of the variance approach, namely Eq. [50] and [51] with calibrated c_3 and Eq. [54] with a "global" value for c_3 (i.e., c_3 =1).

For *LE*, both techniques using specific humidity did not produce reasonable results. The flux-gradient method could not be applied to this desert environment

since the gradients in specific humidity were small, often resulting in countergradient flux conditions. The variance approach using specific humidity (Eq. [52]) was unreliable due to the large uncertainty in the magnitude of the "constants" c_5 and c_6.

An alternative was to solve for *LE* as a residual in the surface energy balance equation, with measurements of net radiation, *Rn*, and soil heat flux, *G*. This is likely to result in more significant discrepancies between measured and estimated *LE* estimates for two reasons. One is that there is an uncertainty in *Rn* and *G* measurements, which is likely to increase the variation in *LE* solved by residual. Second is that *Rn* and *G* measurements reflect a much smaller flux sampling area or flux footprint compared with the turbulent fluxes, *H* and *LE*. For heterogeneous surfaces, such as a desert environment, both factors are found to have a significant effect on the measurement of *Rn* (Kustas et al., 1998) and in providing a representative soil heat flux for an area encompassing the flux footprint (Kustas et al., 2000).

With the best estimates of *H* from the variance method, and measurements of *Rn* and *G*, an example of the comparison with eddy covariance measurements is shown in Fig. 18–4a. In desert environments *LE* is generally less than one-half of *H* during daytime unstable conditions. For this data set the average daytime *H* ~170 W m^{-2} and *LE* ~ 65 W m^{-2}. The RMSE in Fig. 18–4a is ~40 W m^{-2}, which when compared with the average measured *LE* is significant; however, a similar result (with RMSE ~40 W m^{-2}) also is obtained using measured *H* from eddy covariance and solving for *LE* as a residual (Fig. 18–4b). Clearly, in such extreme heterogeneous environments, the uncertainty in *LE* will be more significant than *H* in relation to their relative magnitudes.

CONCLUDING REMARKS

The aerodynamic techniques described here, namely flux-gradient and flux-variance approaches are some of the more common indirect methods for computing turbulent fluxes. Of the two techniques for micrometeorological flux estimation, the variance approach appears to provide more reliable flux estimation across a wide variety of surfaces, particularly for sensible heat. The flux-variance approach is shown to be robust even when measurements are made in the roughness sub-layer (Katul et al., 1999) and do as well as or better than other more complicated indirect methods (Katul et al., 1996; Wesson et al., 2001); however, we presently are unable to resolve the relative influence of all the mechanisms involved in turbulent transport and more importantly we have been unable to develop a unified theory to correct MOST for effects of landscape heterogeneity on mean profiles and turbulent statistics (Roth & Oke, 1995).

The nature of the interactions between the atmosphere and the under lying surface can often be dictated by the uniqueness of different surfaces as well as by the prevailing local micro–meso-scale meteorological conditions. Difficulties encountered in making accurate measurements of mean gradients above the surface, fetch limitations, roughness sub-layer effects, uncertainty in stability correction function formulations, and defining surface roughness parameters impose

significant challenges to the application of the flux-gradient approach. In addition, the fact remains that the flux-gradient relationships only exists for certain conditions; however, in the absence of an alternative approach in land surface modeling (particularly using surface boundary conditions, e.g., Eq. [47], [48], and [49]) flux-gradient relationships thus far presented have served (and to a considerable degree continue to do so) the field with reasonable success over the last three decades. Moreover, for any type of regional assessment of surface fluxes, no other technique is available (Hipps & Kustas, 2000).

REFERENCES

Allen, R.G., M.E. Jensen, J.L. Wright, and R.D. Burman. 1989. Operational estimates of reference evapotranspiration. Agron. J. 81:650–662.

Beljaars, A.C.M., 1982. The derivation fluxes form profiles in perturbed areas. Boundary-Layer Meteorol. 24:35–55.

Boussinesq, J. 1877. Essai sur la théorie des eaux courantes,' Mémories présentés par div. Savants à l.' Acad. Sci. Inst. 23:1–680.

Brost, R.A. 1979. Comments on turbulent exchange coefficients for sensible heat and water vapor under advective conditions. J. Appl. Meteorol. 18:378–380.

Brotezge, J.A., and K.C. Crawford. 2000. Estimating sensible heat flux from the Oklahoma Mesonet. J. Appl. Meteorol. 39:102–116.

Brutsaert, W. 1982. Evaporation into the atmosphere: Theory, history and applications. D. Reidel Publ. Company, Dordrecht, the Netherlands.

Brutsaert, W. 1992. Stability functions in the mean wind speed and temperature in the unstable surface-layer. Geophys. Res. Letters. 19:469–472.

Brutsaert, W., and M. Sugita. 1992. Regional surface fluxes from satellite-derived surface temperatures (AVHRR) and radiosonde profiles. Boundary-Layer Meteorol. 58:355–366.

Businger, J.A. 1966. Transfer of momentum and heat in the planetary boundary layer. p. 305–332. *In* Proc. of the Symp. on Arctic Heat Budget and Atmospheric Circulation, The Rand Corporation. Univ. of California, Berkeley.

Businger, J.A. 1987. A note on the Businger: Dyer profiles. Boundary-Layer Meteorol. 47:145–151.

Businger, J.A., J.C. Wyngaard, Y. Izumi, and E.F. Bradley. 1971. Flux: Profile relationships in the atmospheric surface layer. J. Atmos. Sci. 28:181–189.

Businger, J.A., and A.M. Yaglom. 1971. Introduction to Obukhov's paper on turbulence in an atmosphere with a non-uniform temperature. Boundary-Layer Meteorol. 2:3–6.

Cellier, P., and Y. Brunet. 1992. Flux-gradient relationships above tall plant canopies. Agric. For. Meteorol. 58:93–117.

Chen, F. 1990a. Turbulent characteristics over a rough natural surface: I. Turbulent structures. Boundary-Layer Meteorol. 52:151–175.

Chen, F. 1990b. Turbulent characteristics over a rough natural surface: II. Responses of profiles to turbulence. Boundary-Layer Meteorol. 52:301–311.

Chen, F., and P. Schwerdtfeger. 1989. Flux-gradient relationships for momentum and heat over a rough natural surface. Quart. J. R. Met. Soc. 115:335–352.

Crawford, T.V. 1965. Moisture transfer in free and forced convection. Quart. J. Roy. Meteorol. Soc. 91:18–27.

Deacon, E.L. 1949. Vertical diffusion in the lowest layers of the atmosphere. Quart. J. Roy. Soc. 75:89–103.

Deacon, E.L. 1955. Turbulent transfer of momentum in the lowest layers of the atmosphere. CSIRO Div. of Meteorol. Phys. Tech. Pap. 4:1–36.

Dyer, A.J. 1967. Measurements of evaporation and heat transfer in the lower atmosphere by an automatic eddy-correlation technique. Quart. J. Roy. Meteorol. Soc. 87:401–412.

Dyer, A.J. 1974. A review of flux-profile relationships. Quart. J. Roy. Meteorol. Soc. 96:715–721.

Dyer, A.J. and E.F. Bradley. 1982. An alternative analysis of flux-gradient relationships at the 1976 ITCE. Boundary-Layer Meteorol. 22:3–19.

Dyer, A.J., and B.B. Hicks. 1970. Flux-gradient relationships in the constant flux layer. Quart. J. Roy. Meteorol. Soc. 96:715–721.

Ellison, T.H. 1957. Turbulent transport of heat and momentum from an infinite rough plane. J. Fluid Mech. 2:456–466.

Fick A. 1855. "Uber Diffusion." Ann. Phys. U. Chemie (J.C. Poggendorf) 94:(170)59–86.

Foken, T., and G. Skeib. 1983. Profile measurements in the atmospheric near-surface layer and the use of suitable universal functions for the determination of the turbulent energy exchange. Boundary-Layer Meteorol. 25:55–62.

Garratt, J.R. 1978. Flux profile relations above tall vegetation. Quart. J. Roy. Meteorol. Soc. 104:199–211.

Garratt, J.R. 1980. Surface influences upon vertical profiles in the atmospheric near-surface layer. Quart. J. Roy. Meteorol. Soc. 106:803–819.

Havstad, K.M., W.P. Kustas, A. Rango, J.C. Ritchie, and T.J. Schmugge. 2000. Jornada Experimental Range: A unique arid land location for experiments to validate satellite systems and to understand effects of climate change. Rem. Sensing Environ. 74:13–25.

Hicks, B.B., and R.G. Everett. 1979. Comments on turbulent exchange coefficients for sensible heat and water vapor under advective conditions. J. Appl. Meteorol. 18:371–382.

Hipps, L.E., and W.P. Kustas. Spatial variations in evaporation. p. 105–122. *In* R. Grayson and G. Bloschl (ed.) Spatial patterns in hydrological processes: Observations and modeling. Cambridge Univ. Press., Cambridge.

Högström, U. 1988. Non-dimensional wind and temperature profiles in the atmospheric surface layer: A re-evaluation. Boundary-Layer Meteorol. 42:55–78.

Högström, U. 1996. Review of some basic characteristics of the atmospheric surface layer. Boundary-Layer Meteorol. 78:215–246.

Holzman, B. 1943. The influence of stability on evaporation. Ann. N.Y. Acad. Sci. 44:13–18.

Kader, B.A., and A.M. Yaglom. 1990. Mean fields and fluctuation moments in unstably stratified turbulent boundary layers. J. Fluid Mech. 212:637–662.

Katul, G.G., S.M. Goltz, C. Hsieh, Y. Cheng, F. Mowry, and J. Sigmon. 1995. Estimation of surface heat and momentum fluxes using the flux-variance method above uniform and non-uniform terrain. Boundary-Layer Meteorol. 74:237–260.

Katul, G.G., and C. Hsieh. 1999. A note on the flux-variance similarity relationships for heat and water vapor in the unstable atmospheric surface layer. Boundary-Layer Meteorol. 78:215–246.

Katul, G., C-I. Hsieh, R. Oren, D. Ellsworth, and N. Phillips. 1996. 'Latent and sensible heat flux predictions from a uniform pine forest using surface renewal and flux variance methods. Boundary-Layer Meteorol. 80:249–282.

Katul, G., C-I. Hsieh, and D. Bowling. 1999. Spatial variability of turbulent fluxes in the roughness sub-layer of even-aged pine forest. Boundary-Layer Meteorol. 93:1–28.

Kazanski, A.B., and A.S. Monin. 1956. Izvestia Akad. Nauk. SSSR Geophys. Series 1.

Khanna, S., and J.G. Brasseur. 1997. Analysis of Monin-Obukhov similarity from large-eddy simulation. J. Fluid Mech. 345:251–286.

Kondo, J., and S. Ishida. 1997. Sensible heat flux from the earth's surface under natural convective conditions. J. Atmos. Sci. 54:498–509.

Kustas, W. P., J.H. Prueger, J.L. Hatfield, K. Ramalingam, and L.E. Hipps. 2000. Variability in soil heat flux from a mesquite dune site. Agric. For. Meteorol. 103:249–264.

Kustas, W.P., J.H. Prueger, L.E. Hipps, J.L. Hatfield, and D. Meek. 1998. Inconsistencies in net radiation estimates from use of several models of instruments in a desert environment. Agric. For. Meteorol. 90:257–263.

Lettau, H. 1949. Isotropic and non-isotropic turbulence in the atmospheric surface layer. Geophys. Res. Pap. no. 1:13–84. Air Force Cambridge Res. Lab., Cambridge, MA.

Lumley, J.L., and H.A. Panofsky. 1964. The structure of atmospheric turbulence. Interscience, New York.

McNaughton, K.G., and B.J.J.M. Van den Hurk. 1995. A 'Lagrangian' revision ofthe resistors in the two-layer model for calculating the energy budget of a plant canopy. Boundary-Layer Meteorol. 74:262–288.

McVeil, G.E. 1964. Wind and temperature profiles near the ground in stable stratification. Quart. J. Meteorol. Soc. 90:136–146.

Monin, A.S., and A.M. Obukhov. 1954. Basic laws of turbulent mixing in the ground layer of the atmosphere. Tr. Geofiz. Inst. Akad. Nauk, SSSR no. 24 (151) p. 163–187. *In* (German translation (1958) Sammelband zur Statistischen Theorie der Turulenz H. Goering (ed.) Akademie Verlag, Berlin.

Norman, J.M., W.P. Kustas, and K.S. Humes. 1995. A two-source approach for estimating soil and vegetation energy fluxes from observations of directional radiometric surface temperature. Agric. For. Meteorol. 77:263–293.

Norman, J.M., W.P. Kustas, J.H. Prueger, and G.R. Diak 2000. Surface flux estimation using radiometric temperature: A dual temperature difference method to minimize measurement error. Water Resour. Res. 36:2263–2274.

Obukhov, A.M. 1946. Turbulence in an atmosphere with non-uniform temperature. Tr. Akad. Nauk. SSSR Inst. Teoret. Geofi., no. 1, (English translation in Boundary-Layer Meteorol. 2:7–29, 1971).

Pandolfo, J.P. 1966. Wind and temperature profiles for constant flux boundary layers in lapse conditions with a variable eddy conductivity to eddy viscosity ratio. J. Atmos. Sci. 23:495–502.

Panofsky, H.A. 1961a. An alternative derivation of the diabatic wind profile. Quart. J. R. Met. Soc. 87:109–110.

Panofsky, H.A. 1961b. Similarity theory and temperature structure in the lower atmosphere. Quart. J. R. Met. Soc. 87:597–601.

Panofsky, H.A. 1963. Determination of stress from wind and temperature measurements. Quart. J. Roy. Meteorol. Soc. 89:85–94.

Panofsky, H.A., A.K. Blackadar, and G.E. McVehil. 1960. The diabatic wind profile. Quart. J. Roy. Meteorol. Soc. 86:390–398.

Panofsky, H., and J. Dutton. 1984. Atmospheric turbulence: Models and methods for engineering applications. John Wiley & Sons, New York.

Paulson, C.A. 1970. The mathematical representation of wind speed and temperature profiles in the unstable atmospheric surface layer. J. Appl. Meteorol. 9:857–861.

Prandtl, L. 1904. 'Uber Flüssigkeitsbewegung bei sehr kleiner Reibung', Verhandl. III, Internat. Math.- Kong., Heidelberg, Teubner, Leipzig. p. 484–491. (1905) (Also in Gesammelte Abhundlungen, Vol. 2, Springer-Verlag, Berlin, 1961, p. 575–584. English in NACA, Tech. Mem. no. 452).

Pruitt, W.O., D.L. Morgan, and F.J. Lourence. 1973. Momentum and mass transfers in the surface boundary layer. Quart. J. Roy. Meteorol. 99:370–386.

Raupach, M.R. 1979. Anomalies in flux-gradient relationships over forest. Bound.-Layer Meteorol. 16:467–486.

Raupach, M.R. 1992. Drag and drag partition on rough surfaces. Boundary-Layer Meteorol. 60:375–395.

Raupach, M.R. 1994. Simplified expression for vegetation roughness lengths and zero-plane displacement as functions of canopy height and area index. Boundary-Layer Meteorol. 71:211–216.

Raupach, M.R. 1995. Corrigenda. Boundary-Layer Meteorol. 76:303–304.

Raupach, M.R., R.A. Antonia, and S. Rajagopalan. 1991. Rough-wall turbulent boundary layers. Appl. Mech. Rev. 44:1–25.

Raupach, M.R., A.S. Thom, and I. Edwards. 1980. Wind tunnel study of turbulent flow close to regularly arrayed rough surfaces. Bound.-Layer Meteorol. 18:373–397.

Richardson, L.F. 1920. The supply of energy from and to atmospheric eddies. Proc. Roy. Soc. London A97:354–373.

Roth, M., and T.R. Oke. 1995. Relative efficiencies of turbulent transfer of heat, mass, and momentum over a patchy urban surface. J. Atmos. Sci. 52:1863–1874.

Schmid, H.P., and B. Bunzli. 1995. The influence of surface texture on the effective roughness length. Quart. J. Roy. Meteorol. Soc. 121:1–21.

Schmidt, W. 1917. 'Der Massenaustauch bei der ungeordneten Strömung in freier Luft und seine Folgen' Sitzber, Kais. Akad. Wissen. Wien [2a] 126:757–804.

Sellers, W.D. 1962. A simplified derivation of the diabatic wind profile. J. Atmos. Sci. 19:180.

Stull, R. 1988. An introduction to boundary layer meteorology. Kluwer Academic Publ., Boston.

Sugita, M., T. Hiyama, N. Endo, and S.-F. Tian. 1995. Flux determination over a smooth surface under strongly unstable conditions. Bound.-Layer Meteorol. 73:145–158.

Sun, J., and L. Mahrt. 1995. Determination of surface fluxes from the surface radiative temperature. J. Atmos. Sci. 52:1096–1106.

Swinbank, W.C. 1960. Wind profile in thermally stratified flow. Nature 186(4723):463–464.

Swinbank, W.C. 1964. The exponential wind profile. Quart. J. Roy. Meteorol. Soc. 90:119–135.

Swinbank, W.C. 1968. A comparison between predictions of dimensional analysis for the constant-flux layer and observations in unstable conditions. Quart. J. Roy. Meteorol. Soc. 94:460–467.

Taylor, G.I. 1915. Eddy motions in the atmosphere. Phil. Trans. Roy. Soc. Lond., A215:1–26.

Tennekes, H. 1973. The logarithmic wind profile. J. Atmos. Sci. 30:234–238.

Thom, A.S. 1971 Momentum absorption by vegetation. Quart. J. Roy. Meteorol. Soc. 97:414–428.

Thom, A.S. 1975 Momentum, mass and heat exchange of plant communities. p. 57–109. *In* J.L. Monteith (ed.) Vegetation and the atmosphere. Vol. I. Principles. Academic Press, London.

Tsvang, L.R., V.P. Kukharts, and V.G. Perepelkin.1998. Atmospheric turbulence characteristics over a temperature-inhomogeneous land surface: Part II. The effect of small-scale inhomogeneities of surface temperature on some characteristics of the atmospheric surface layer. Bound.-Layer Meteorol. 8:103–124.

Verhoef, A., H.A.R. de Bruin, and B.J.J.M. Van Den Hurk. 1997. Some practical notes on the parameter kB^{-1} for sparse vegetation. J. Appl. Meteorol. 36:560–572.

Verma, S.B., N.J. Rosenberg, and B.L. Blad. 1978. Turbulent exchange coefficients for sensible heat under advective conditions. J. Appl. Meteorol. 17:330–338.

Warhaft, Z. 1976. Heat and moisture flux in the stratified boundary layer. Quart. J. Roy. Meteorol. Soc. 102:703–707.

Webb, E.K. 1960. An investigation of the evaporation from Lake Eucumbene. CSRIO Aust. Div. Meteorol. Phys. Tech. Pap. no.10. CSRIO, Melbourne, Australia.

Webb, E.K. 1970. Profile relationships: The log-linear range, and extension to strong stability. Quart. J. Roy. Meteorol. Soc. 96:67–90.

Webb, E.K. 1982. Profile relationships in the superadiabatic surface layer. Quart. J. Roy. Meteorol. Soc. 108:661–688.

Wesson, K.H., G. Katul, and C-T. Lai. 2001. Sensible heat flux estimation by flux variance and half-order time derivative methods. Water Resour. Res. 37(9):2333–2343.

Wieringa, J. 1986. Roughness-dependent geographical interpolation of surface wind speed averages. Quart. J. Roy. Meteorological Soc. 112:867–889.

Williams, A.G., and J.M. Hacker. 1993. Interactions between coherent eddies in the lower convective boundary layer. Boundary-Layer Meteorol. 64:55–74.

Wyngaard, J.C., O.R. Cote, and Y. Izumi. 1971. Local free convection, similarity and the budgets of shear stress and heat flux. J. Atmos. Sci. 28:1171–1182.

Yaglom, A.M. 1977. Comments on wind and temperature flux-profile relationships. Boundary-Layer Meteorol. 11:89–102.

Yamamoto, G. 1959. Theory and transport in non-neutral conditions. J. Meteorol. Soc., Japan, 37:60–70.

Yamamoto, G. 1975. Generalization of the KEYPS formula in diabatic conditions and related discussion on the critical Richardson number. J. Meteorol. Soc. Japan 53:189–194.